

Article

Trends of Ground-Level Ozone in New York City Area during 2007–2017

Subraham Singh  and Ilias G. Kavouras * 

Department of Environmental, Occupational and Geospatial Health Sciences, City University of New York Graduate School of Public Health and Health Policy, 55 West 125th Street, New York, NY 10027, USA; subraham.singh25@sph.cuny.edu

* Correspondence: ilias.kavouras@sph.cuny.edu

Abstract: The spatiotemporal patterns of ground level ozone (O_3) concentrations in the New York City (NYC) metropolitan region for the 2007–2017 period were examined conjointly with local emissions of O_3 precursors and the frequency of wildfires. Daily 8-h and 1-h O_3 and nitric oxide (NO) concentrations were retrieved from the US Environmental Protection Agency (EPA) Air Data. Annual emission inventories for 2008 and 2017 were acquired from EPA National Emissions Inventory (NEI). The number and area burnt by natural and human-ignited wildfires were acquired from the National Interagency Fire Center (NIFC). The highest daily 8-h max O_3 concentrations varied from 90 to 111 parts per billion volume (ppbv) with the highest concentrations measured perimetrically to NYC urban agglomeration. The monthly 8-h max O_3 levels have been declining for most of the peri-urban sites but increasing (from +0.18 to +1.39 ppbv/year) for sites within the urban agglomeration. Slightly higher O_3 concentrations were measured during weekend than those measured during the weekdays in urban sites probably due to reduced O_3 titration by NO. Significant reductions of locally emitted anthropogenic nitrogen oxides (NO_x) and volatile organic compounds (VOCs) may have triggered the transition from VOC-limited to NO_x -limited conditions, with downwind VOCs sources being critically important. Strong correlations between the monthly 8-h max O_3 concentrations and wildfires in Eastern US were computed. More and destructive wildfires in the region were ignited by lightning for years with moderate and strong La Niña conditions. These findings indicate that climate change may counterbalance current and future gains on O_3 precursor's reductions by amending the VOCs-to- NO_x balance.

Keywords: annual trend; day-of-the-week variation; ozone precursors; urban environment; wildfires



Citation: Singh, S.; Kavouras, I.G. Trends of Ground-Level Ozone in New York City Area during 2007–2017. *Atmosphere* **2022**, *13*, 114. <https://doi.org/10.3390/atmos13010114>

Academic Editor: Giacomo Alessandro Gerosa

Received: 26 December 2021

Accepted: 10 January 2022

Published: 12 January 2022

Publisher's Note: MDPI stays neutral with regard to jurisdictional claims in published maps and institutional affiliations.



Copyright: © 2022 by the authors. Licensee MDPI, Basel, Switzerland. This article is an open access article distributed under the terms and conditions of the Creative Commons Attribution (CC BY) license (<https://creativecommons.org/licenses/by/4.0/>).

1. Introduction

Ground-level ozone (O_3) negatively impacts human health across life stages, natural ecosystems, and climate [1,2]. Ozone is a strong oxidative agent that reacts with proteins and lipids in the airways lining fluid of the lung and compromised lung function [3–5]. Early-life exposure to O_3 affects the growth and function of developing lungs and may promote the asthma phenotype in the first year of life [6–8]. Children exposed to O_3 are also more likely to have airway hyper responsiveness [9]. O_3 exposures have been consistently shown to increase asthma medication use, mortality, emergency department (ED) visits, and hospitalizations by exacerbating asthma and chronic obstructive pulmonary disease (COPD) [1,10].

O_3 , a secondary pollutant, is produced from the daytime oxidation of irradiated mixtures of volatile organic compounds (VOCs) and nitrogen oxides (NO_x) ($NO + NO_2 = NO_x$) (precursors, thereafter). O_3 levels increase as VOCs levels increase, while increasing NO_x levels may either generate or titrate O_3 depending on instantaneous VOC/ NO_x ratio (in parts per million carbon (ppmC)/parts per million (ppm)) [11]. VOCs and NO_x are emitted from fossil and contemporary fuel combustion in anthropogenic activities and wildfires.

Isoprene and terpenes are the predominant biogenic VOCs released by vegetation. O₃ concentrations vary from 20–40 ppbv in remote continental areas up to 100–200 ppbv in areas downwind of metropolitan urban areas [12]. On a local scale, there is a strong spatiotemporal gradient of O₃ levels with the lowest concentration being measured at the proximity of combustion sources (e.g., downtown or city center) when O₃ is titrated by nitric oxide (NO), and the highest O₃ levels at downwind locations in the late afternoon [13].

Because ambient O₃ levels are regulated by the National Ambient Air Quality Standards (NAAQS) pursuant to the Clean Air Act (CAA) and its amendments, strategies, and measures to reduce both VOCs and NO_x emissions from anthropogenic sources have been implemented over the past four decades [14]. As a result, ambient O₃ levels declined considerably in many heavily O₃ polluted areas but reached a plateau and in many urban and peri-urban areas is trending upwards, lately [15]. Changes in local meteorology did not account for O₃ trends in urban and continental background locations [16]. On a global and regional scale, increasing emissions of VOCs and NO_x in developing countries amplified background O₃ concentrations [17]. More frequent and intense wildfires, amplified by climate change, are also linked to episodic events of high O₃ pollution in downwind locations [18,19]. Lastly, spatiotemporal changes of NO_x and VOCs emissions and their relative abundance may also contribute to the observed positive trends as the intensity of O₃ destruction by NO titration is declining and more VOCs will increase O₃ [15].

The New York-Newark-Jersey City, NY-NJ-PA Metro Area is the largest and most populous in North America (area of 17,314 km² and 19,216,182 residents in 2020) [20]. It encompasses New York City (NYC), Long Island, Mid and Lower Hudson Valley, and major urban areas in New Jersey. The region is a moderate non-attainment area exceeding the 2015 NAAQS O₃ standard of 70 ppbv [21]. The aims of this study were (i) to characterize the spatial and temporal variation of O₃ in the NYC region using quantitative statistical tools and (ii) to investigate the impact of local emissions trends and wildfires on O₃ levels, with the overall objective of delineating the atmospheric conditions and sources at local and regional scale contributing to O₃ pollution in NYC.

2. Materials and Methods

2.1. Air Pollution Data Acquisition and Processing

Daily 8-h max O₃ measurements at sixteen (16) sites in the New York City metropolitan region for the 2007–2017 period were retrieved from the U.S. Environmental Protection Agency (USEPA) Air Data system (Table 1) [22]. In addition, hourly O₃ and nitric oxide (NO) concentrations were obtained for sites with concurrent measurements for the monitoring period. Figure 1 shows the locations of the air quality monitoring sites, population, and major traffic corridors. There were:

- Seven sites are operated by the New York State Department of Environmental Conservation, four of them within NYC (City College of New York in West Harlem) (#1), Pfizer Lab in Bronx (#3) and Queens College in Queens (#4), with more than 1.5 million of people within 8 km of each site; White Plains in Westchester (#6, about 450,000 residents within 8 km) County in Figure 1 and three of them in Suffolk County, Long Island (#10, #11 (500,000–700,000 people) and #12 (57,000 people) in Figure 1);
- Six sites were operated by the New Jersey Department of Environmental Protection. Three of the sites (#2, #5 and #15) were in populated urban settings (from 600,000 to 2,500,000 people within 8-km radius), while the remaining three were further away from New York City (#13, #14 and #16, less than 275,000 people within 8-km); and
- Three sites along the US Interstate-95 highway to Bridgeport, CT, operated by the Connecticut Department of Environmental Quality (#7, #8, and #9 in Figure 1, with 180,000 to 280,000 people living within an 8-km radius).

Ambient O₃ concentrations were photometrically measured with approved federal equivalent methods.

Table 1. The characteristics (ID #, name, type, latitude, longitude, elevation, distance to CCNY site, and population within an 8-miles radius of O₃ monitoring sites in the study area.

ID #	Site Name	Latitude (°N)	Longitude (°W)	Elevation (m)	Distance from CCNY Site (km)	Population (<8 km)
NYC urban sites						
1	CCNY	40.819	73.948	45	-	4,117,668
2	Leonia	40.870	73.991	1	6.7	2,675,227
3	Pfizer Lab Site ^a	40.867	73.878	31	7.8	2,900,231
4	Queens College ^a	40.736	73.821	25	13.9	2,825,439
5	Bayonne ^a	40.670	74.126	3	22.5	1,426,212
Peri-urban sites						
6	White Plains	41.051	73.763	64	31.5	452,018
7	Greenwich Point Park	41.004	73.585	3	37.5	283,192
8	Sherwood Island ^a	41.118	73.336	4	62.4	188,692
9	Stratford	41.152	73.103	3	79.5	288,077
10	Babylon	40.745	73.419	27	45.2	671,479
11	Holtsville	40.827	73.057	45	75.2	455,965
12	Riverhead	40.960	72.712	31	105.7	57,381
13	Ramapo	41.058	74.255	3047	37.8	265,429
14	Chester ^a	40.787	74.676	278	61.3	205,712
15	Rutgers University Monmouth University	40.462	74.429	19	56.6	619,552
16	University	40.277	74.005	8	60.5	240,959

^a Hourly O₃ and NO measurements were retrieved.

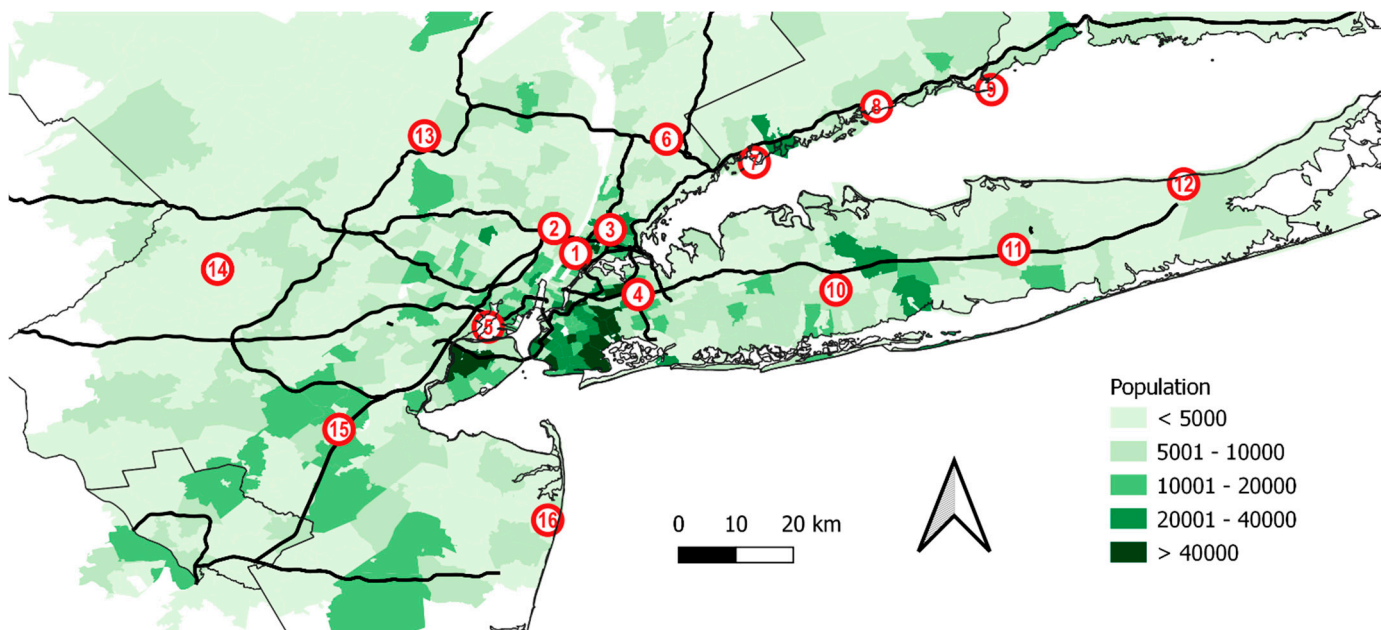


Figure 1. The locations of air quality sites, 2019 population (by US Census track [20]) and primary road network in the study area. The numbers in the circle refer to sites ID# in Table 1.

2.2. Emissions Inventories and Wildfires

The 2008 and 2017 NO_x and VOCs emissions for New York, New Jersey, and Connecticut were obtained from the USEPA National Emissions Inventory (NEI). It includes emissions from point, area, mobile (on- and off-road), and event-specific sources based on source activity data provided by the state, local, and tribal air agencies through the Emissions Inventory System (EIS). Emissions have been reported by EIS sectors since 2008 as described in the Source Classification Codes (SCCs). SCCs are source-specific processes

or functions that emit air pollutants. For this study, 2008 and 2017 NEI data by EIS sectors were grouped into fourteen source types as follows: agriculture/livestock waste; biogenics (including vegetation and soil); bulk gasoline terminals; commercial cooking; fires (including agricultural, prescribed, and wildfires); commercial, electrical generation, industrial and residential fuel combustion; gas stations; industrial and non-industrial processes; mobile sources, solvent fugitive emissions; and waste disposal. The number of human- and lightning-ignited wildfires and area burnt for the 2007–2017 period by year for each of the eleven Geographic Area Coordinating Group (GACG) were obtained from the National Interagency Fire Center (NIFC) [23]. The study area is part of the Eastern Area Coordination Center (EACC) that includes a total of twenty (20) states: Connecticut, Delaware, Illinois, Indiana, Iowa, Maine, Massachusetts, Maryland, Michigan, Minnesota, Missouri, New Hampshire, New Jersey, New York, Ohio, Pennsylvania, Rhode Island, Vermont, West Virginia, and Wisconsin.

2.3. Data Analysis

Ambient daily 8-h max O₃ concentrations were tested for normality using the Shapiro-Wilk test. The significance of difference among sites was assessed with the non-parametric Kruskal-Wallis at $\alpha = 0.05$. The daily 8-h max O₃ absolute (ΔC) and the percent relative ($\% \Delta C / \text{Ref}$) concentration differences and the coefficient of divergence (COD) were computed [24]. The CCNY (located in City College of New York) (Site #1 in Figure 1) was the reference site because of its central location to the study area. COD values vary from 0 to 1, with high COD values being indicative of spatial gradient. The paired ΔC between two sites were used to determine whether concentrations change simultaneously among the sites over time. The $\% \Delta C / C_{\text{Ref}}$ of 24-h paired concentration was computed to assess systematic differences between the sites and site-to-site variation, respectively [24]. COD was used to assess the spatial uniformity of measurements with respect to the concentration levels [25].

The monthly 8-h max O₃ concentration was computed for months with more than 75% of daily 8-h max O₃ measurements. It has been previously used to examine the effect of wildfires on O₃, compliance with NAAQS, and to smooth the effects of local meteorology and short-term changes in local emissions [24,25]. The annual trend was computed using the de-seasonalized monthly 8-h max O₃ concentrations by applying the non-parametric sequential Mann-Kendall test at a confidence level of 95% [26,27].

Hourly NO and O₃ concentrations were used to compute the morning NO-O₃ crossover time (t_{NOxO_3}) (in h) and the O₃ accumulation time ($t_{\text{O}_3\text{-acc}}$) (in h) as follows: (i) the t_{NOxO_3} is the time of the day where NO and O₃ profiles intersected after the early morning NO peak; and (ii) the $t_{\text{O}_3\text{-acc}}$ is the time of the day with the highest O₃ concentration [11]. The ozone accumulation rate (in ppbv O₃/h) was computed as follows:

$$\text{Acc.Rate} = ([\text{O}_3]_{t_{\text{O}_3\text{-acc}}} - [\text{O}_3]_{t_{\text{NOxO}_3}}) / (t_{\text{O}_3\text{-acc}} - t_{\text{NOxO}_3})$$

where $[\text{O}_3]_{t_{\text{NOxO}_3}}$ and $[\text{O}_3]_{t_{\text{O}_3\text{-acc}}}$ are the O₃ concentrations at NOxO₃ crossover and O₃ accumulation times of the day, respectively.

The two-tailed Spearman correlation coefficient was computed to assess the relationship between wildfires and annual 8-h max O₃ concentration. Analyses were done using SPSS (Version 26) (IBM Analytics, Armonk, NY, USA) and Origin Pro (version 9.1) (Origin Lab, Northampton, MA, USA).

3. Results

3.1. Spatial and Temporal Trends

Figure 2 shows the time series of monthly 8-h max O₃ at the sixteen sites. Monthly 8-h max O₃ levels at all sites ranged from a 25 ppbv during the winter months (December to February) to 90 at Pfizer Lab (#3), 91 ppbv at CCNY (#1) and Riverside (#12), 95 ppbv at Leonia (#2), 94 ppbv at Ramapo (#), 96 ppbv at Queens College (#4), Holtsville (#11) and Chester (#14), 97 ppbv at Monmouth University (#16), 101 at White Plains (#6), 102 ppbv

at Rutgers Univ (#15), 103 ppbv at Stratford (#8) and Sherwood Island (#9), 105 ppbv at Greenwich Point (#7), 111 ppbv in Bayonne (#5) and 114 ppbv in Babylon (#10). The highest monthly O_3 mixing ratios were typically measured in June and July. Note that O_3 was measured during April–October at Riverhead in NY, Ramapo and Monmouth University in NJ, and all three sites in Connecticut.

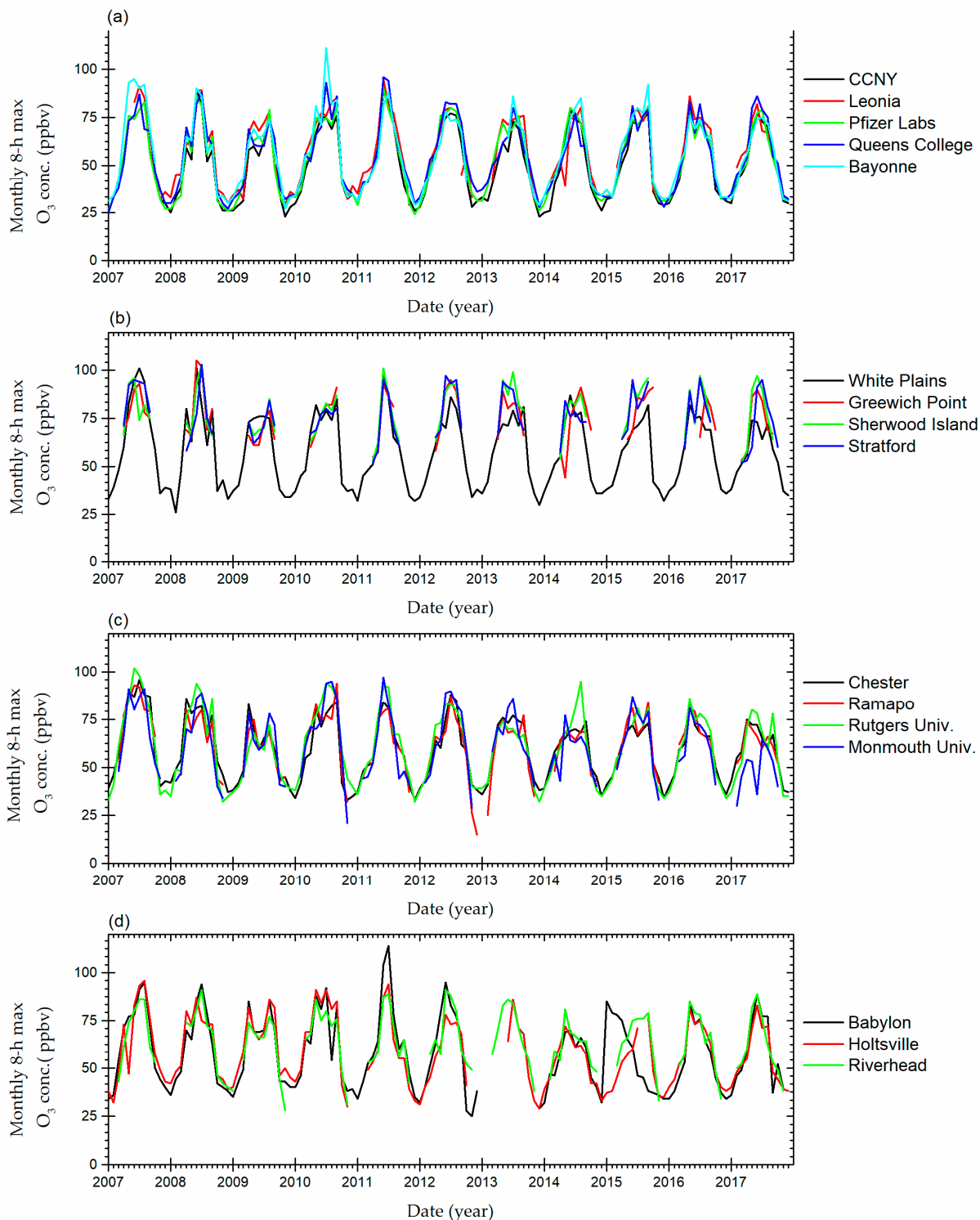


Figure 2. Times series of monthly 8-h max O_3 (in ppbv) at (a) urban sites; (b) peri-urban sites north of NYC and in Connecticut; (c) peri-urban sites in NJ and (d) peri-urban sites in Long Island.

Table 2 shows the 2017 8-h max O₃ concentration (in ppbv), the site-specific COD value, median (and standard deviation (σ)) of absolute (ΔC) and relative (%ΔC/Ref) concentration differences (relative to CCNY air quality monitoring site) and the annual trends of monthly 8-h max O₃ levels for each site (ppbv/year). The 8-h maximum O₃ concentrations for 2017 varied from 60 ppbv for the coastal site upwind of New York City in Monmouth University (#16) to 81 ppbv for the two coastal sites downwind of New York City in Connecticut (Sherwood Island (#8) and Stratford (#9)). The sites were grouped in two clusters based on spatiotemporal similarities to the reference site (#1 at CCNY in Manhattan). The first cluster was composed of sites within the NYC urban area (#3–5), with low COD values (from 0.10 to 0.14), ΔC (2–4 ppbv) and %ΔC/C_{ref} (from 6 to 12%) indicating the lack of a spatial gradient within the densely populated area. For most of these sites (except for Bayonne (#5) that is located on the south of the densely NYC populated area), the 8-h max O₃ concentrations were increasing from 0.18 to 1.39 ppbv/year. For sites located perimetrically to NYC, slightly higher COD (from 0.13 to 0.22), ΔC (from 5 to 9 ppbv) and %ΔC/C_{ref} (from 16 to 26%) suggested a weak spatial trend particularly across the west-east axis relative to NYC. The 8-h max O₃ concentrations declined from −0.25 to −1.82 ppbv/year except for two of the nearest to NYC sites in Connecticut from +0.03 (#7) and +0.43 (#8) ppbv/year.

Table 2. The 2017 8-h max O₃ concentration, mean COD, median (and standard deviation (σ)) of absolute (ΔC) and relative (%ΔC/Ref) concentration differences (compared to CCNY site) and annual trends of 8-h max O₃ concentrations.

Site No and Location	2017 8-h Max O ₃ (ppbv)	COD	ΔC (Median (σ))	%ΔC/C _{ref} (Median (σ))	Annual Trend (ppbv/year)
NYC urban sites					
1 CCNY	70	n.c.	n.c.	n.c.	0.24 *
2 Leonia	74	0.12	4 (5.0)	11 (129.7)	1.39 **
3 Pfizer Laboratories	69	0.10	2 (3.8)	6 (107.3)	0.31 **
4 Queens College	79	0.14	4 (5.1)	12 (119.1)	0.18
5 Bayonne	67	0.12	2 (5.2)	7 (108.1)	−0.28
Peri-urban sites					
6 White Plains	72	0.18	6 (6.6)	21 (92.5)	−0.25 *
7 Greenwich Point Park	74	0.14	8 (6.4)	20 (32.4)	0.03 ^a
8 Sherwood Island	81	0.13	7 (7.3)	18 (30.1)	0.43 ^{*,a}
9 Stratford	81	0.16	9 (7.7)	23 (38.4)	0.01 ^a
10 Babylon	77	0.19	6 (7.3)	20 (161.4)	−0.69 **
11 Holtsville	71	0.22	7 (12.0)	23 (199.1)	−1.82 **
12 Riverhead	76	0.19	8 (8.9)	23 (102.9)	−0.41 **
13 Ramapo	66	0.16	5 (9.0)	16 (164.2)	0.01 ^a
14 Chester	70	0.22	8 (8.1)	27 (150.2)	−0.82 **
15 Rutgers University	75	0.20	8 (6.7)	26 (142.4)	−0.41 *
16 Monmouth University	60	0.17	6 (9.0)	18 (154.2)	−0.73 **

n.c.: not computed. ^a Data available only from April to October. * $p < 0.05$, ** $p < 0.001$.

Figure 3 shows the mean ($\pm 3 \times$ standard error) ozone weekend-to-weekday effect (OWE) ratio of average maximum O₃ concentrations for each site. OWE values higher than one indicate that weekend O₃ concentrations were higher than those measured during the weekdays. For all NYC urban sites, the OWE ratio was higher than 1 (from 1.04 to 1.07), indicating that weekend O₃ levels were higher than those measured during weekend. For two of the most populated peri-urban sites (White Plains (#6) and Babylon (#10)), the OWE ratio was also higher than 1 (1.02 and 1.03, respectively), and less than one for the remaining peri-urban sites.

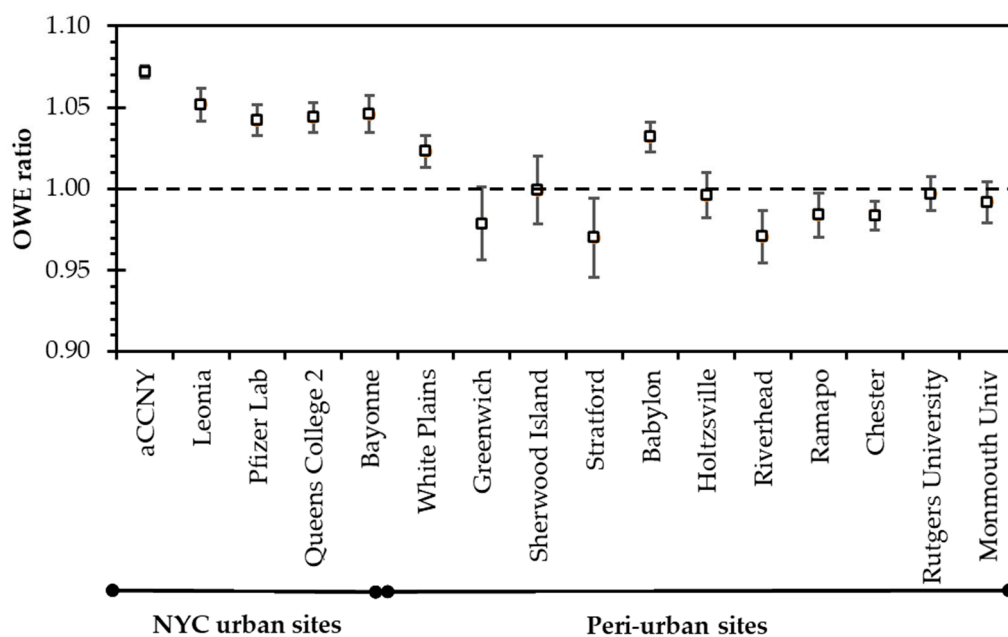


Figure 3. The mean ($\pm 3 \times$ standard error) ozone weekend-to-weekday effect (OWE) ratio of average maximum O₃ concentrations for each site.

Figure 4 presents the day-of-week variation of the morning NO_xO₃ crossover time (t_{NOxO3}), the O₃ accumulation time (t_{O3_acc}) and the O₃ accumulation rate for (a) Queens College (NYC urban site (#4)) and (b) Chester (peri-urban site (#14)). For Queens College site, the t_{NOxO3} crossover was observed at between 7:00 and 9:00 am and O₃ accumulated for six hours during weekdays and Saturday (Figure 4a). During Sunday, O₃ formation was not hampered because of low NO levels. The weekend NO concentrations (24-h mean: 1.4–1.8 ppbv; 1-h max: 3.7–6.9 ppbv) was up to three times lower than that measured during weekdays (24-h mean: 2.7–3.4 ppbv; 1-h max: 7.7–14.0 ppbv). The lowest accumulation rate observed on Sunday (1.24 ppbv/h) was counterbalanced by the longer accumulation period, resulting in elevated O₃ concentrations. Because of the lack of titration in the early morning, the O₃ overnight carryover on weekend (1-h: 18.6–23.4 ppbv) was higher than that during weekdays (1-h: 13–16.7 ppbv), adding to higher O₃ concentrations in weekend.

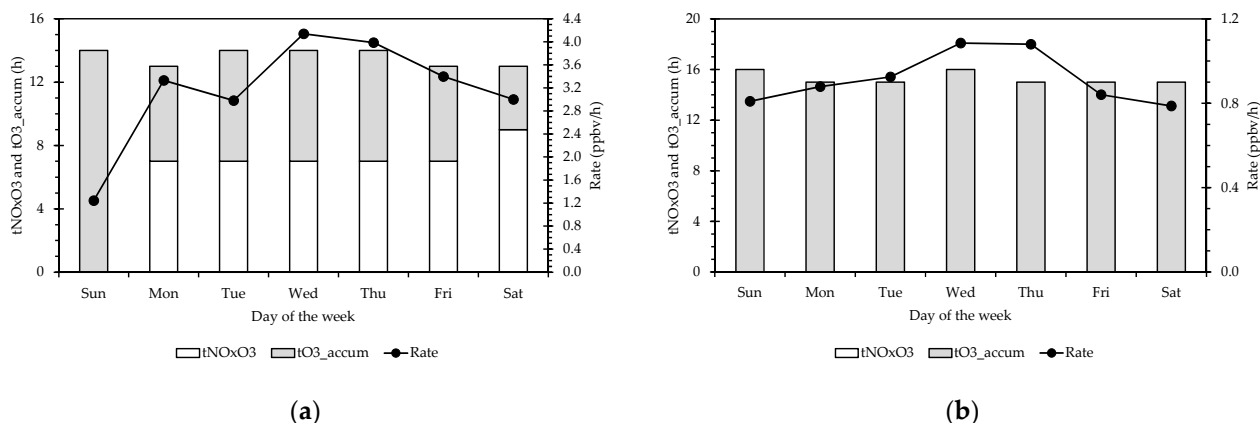


Figure 4. The day-of-week variation of the morning NO-O₃ crossover time (t_{NOxO3}), the O₃ accumulation time (t_{O3_acc}) (h), and the O₃ accumulation rate (ppbv/h) for (a) Queens College (Site #10) and (b) Chester (Site #4).

For Chester (Figure 4b), NO levels were minimal during weekends (1-h max levels < 0.2 ppbv) and less than 1 ppbv during weekdays. As such, there was no O₃

titration, with prolonged periods of ozone accumulation albeit at low accumulation rates (0.81–1.08 ppbv/h) for both weekends and weekdays. Moreover, the O₃ overnight carry-over (28.5–31.3 ppbv) did not vary among different days of the week.

3.2. O₃ Precursors Emissions and Wildfires

Figure 5 shows the emission fraction (source category emission divided by the total emissions) of NO_x and VOCs emissions in 2008 and 2017 in fifteen categories including anthropogenic combustion processes, wildfires, and biogenic emissions. In total, NO_x emissions declined from 766,498 tons in 2008 to 89,209 tons in 2017. VOCs emissions also significantly declined, from 1,341,849 tons in 2008 to 213,272 tons in 2017. However, the relative abundance of source categories on both NO_x and VOCs remained unchanged. Biogenic (e.g., isoprene, terpenes) VOCs was the predominant source (approximately 40% in 2008 and above 50% in 2017) followed by combustion-related mobile sources (about 30% in 2008 and less than 20% in 2017) and fugitive solvent emissions (about 20% for 2008 and 2017). For NO_x, mobile emissions (more than 76.5%) dominated both 2008 and 2017 emissions with minor quantities from other fossil and contemporary fuel sources (Figure 5b). These trends were consistent with the declining NO_x levels. VOCs levels may also decrease albeit the chemical content may have been moderately altered.

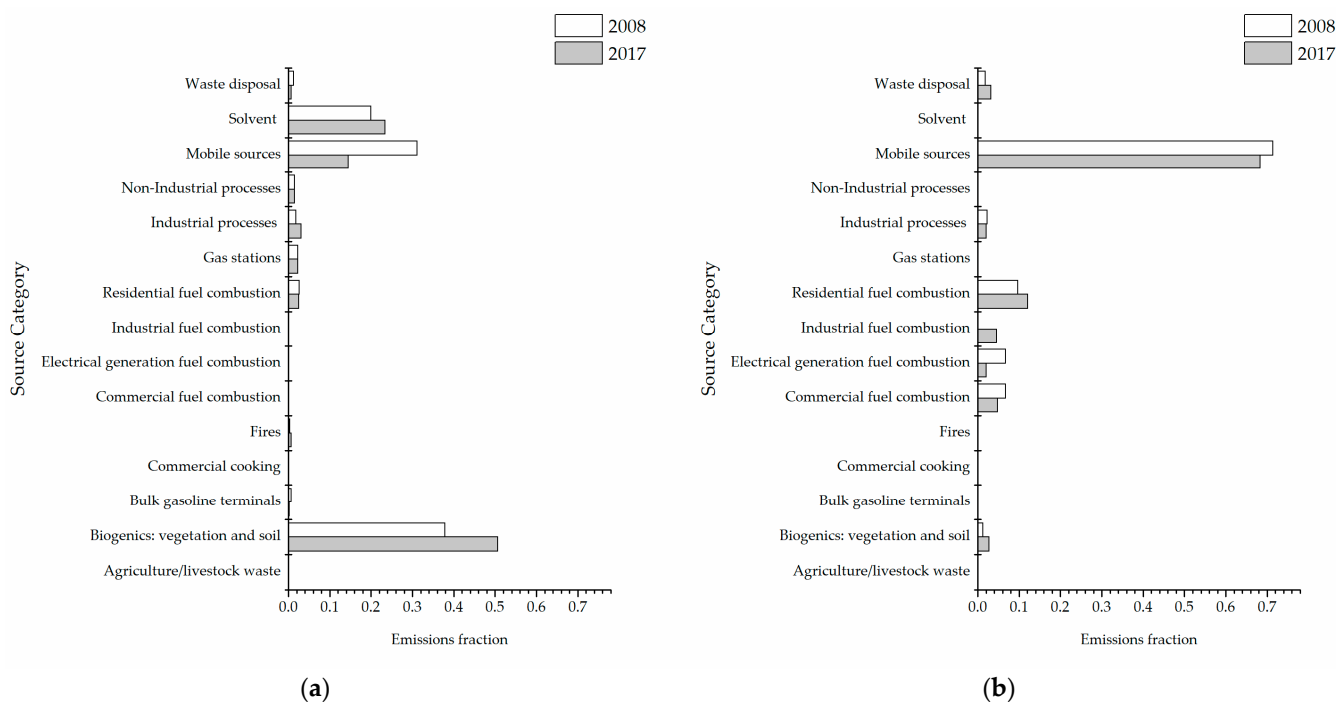


Figure 5. The relative abundance of (a) VOCs and (b) NO_x by source category in NY, NJ and CT in 2008 and 2017.

Table 3 shows the Spearman correlation coefficient of O₃ concentrations, the number of and area burnt by fires within the areas managed by the ten GACC coordinating centers. Moderate to strong correlations were computed for the number (0.91, $p < 0.001$) and area (0.60, $p = 0.01$) burnt by lightning-ignited fires in the Eastern Area followed by fires in the Southern Area coordination center (number: 0.80, $p = 0.003$) encompassing all states east of the Mississippi River and adjacent westerly states. Weaker correlations were computed for human-ignited wildfires in the same regions. It is noteworthy that prescribed burns in winter and spring for ecological management and to manage biomass fuel on the forest floor account for most of the human-induced fires in the Southern area. The Spearman correlation coefficient declined for wildfires further away from the study area

Table 3. Spearman correlation coefficients of monthly 8-h max O₃ concentrations and lightning, the number and area burnt by human-induced wildfires in regional GACG coordinating centers.

GACG Coordinating Centers *	Number		Area Burnt	
	Lightning	Human	Lightning	Human
Eastern Area	0.91 ***	0.47	0.60	0.58
Southern Area	0.80 **	0.24	0.44	0.41
Northern Rockies	0.00	0.08	0.36	0.31
Southwest	0.46	0.06	−0.11	0.18
Rocky Mountain	0.41	0.25	0.44	0.19
Great Basin	0.16	0.35	0.34	0.36
Northwest	−0.48	−0.29	−0.08	−0.10
Northern California	−0.12	−0.61	0.06	−0.32
Southern California	0.17	0.36	0.39	0.16
Alaska	0.01	−0.12	−0.28	−0.32

* Eastern Area (Connecticut, Delaware, Illinois, Indiana, Iowa, Massachusetts, Maryland, Maine, Michigan, Minnesota, Missouri, New Hampshire, New Jersey, New York, Ohio, Pennsylvania, Rhode Island, Vermont, Wisconsin, and West Virginia); Southern Area (Virginia, North Carolina, South Carolina, Georgia, Florida, Kentucky, Tennessee, Alabama, Mississippi, Louisiana, Arkansas, Oklahoma except for Panhandle, Central and Eastern Texas); Northern Rockies (North Dakota, Montana and Idaho-north of the Salmon River, Yellowstone National Park, and a small portion of South Dakota); Southwest (Western Texas, New Mexico, and Arizona except for the Strip); Rocky Mountain (Kansas, Nebraska, North Dakota, Colorado, and Wyoming except for western Wyoming mountains); Great Basin (Utah, Nevada, Idaho-south of the Salmon River, the western Wyoming mountains, and the Arizona Strip); Northwest (Washington and Oregon). ** Correlation is significant at the 0.01 level (two-tailed) *** Correlation is significant at the 0.001 level (two-tailed).

The annual variation of 8-h max O₃ concentration, number and area burnt by lightning-ignited wildfires in the Eastern and Southern GACG areas are presented in Figure 6a,c,d. Figure 6b also shows the Oceanic Niño Index (ONI), the 3-month moving average sea surface temperature anomaly of the east-central tropical Pacific, near the International Dateline. ONI values > +0.5 are indicative of El Niño conditions, while ONI values < −0.5 °C are characteristic of La Niña conditions. Overall, there were more naturally occurring wildfires in the Eastern and Southern area during La Niña periods in 2007–2008, 2010–2011 and recently, than years with El Niño conditions.

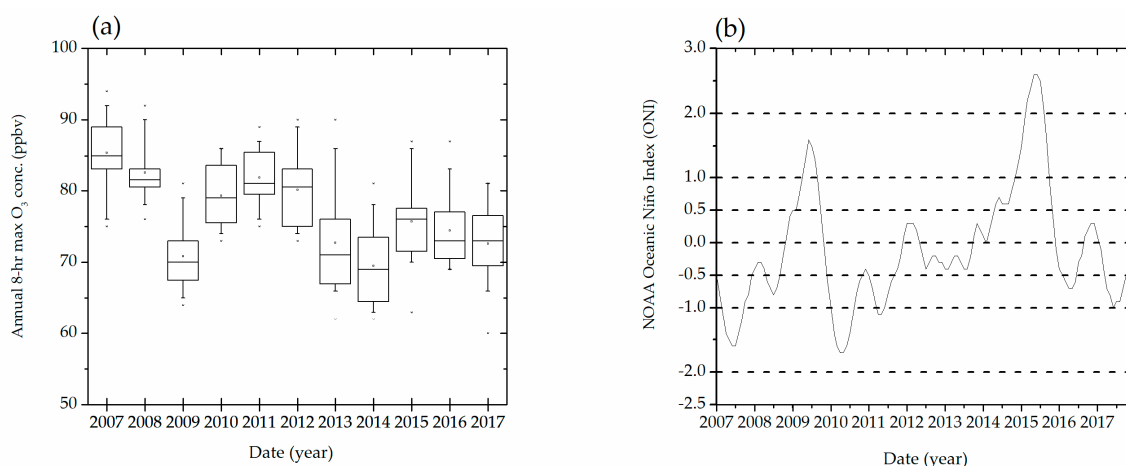


Figure 6. Cont.

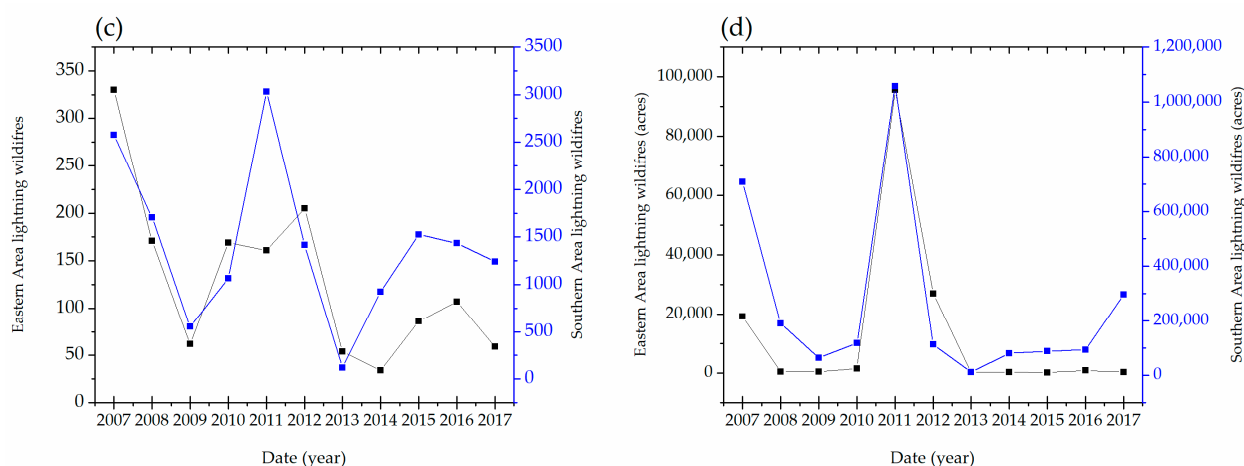


Figure 6. The (a) monthly 8-h max O_3 concentrations at the study area; (b) temperature abnormalities; (c) the number and (d) are burnt by wildfires in the Eastern and Southern areas during the period 2007–2017.

4. Discussion

In this study, we observed heterogeneity in the trends of monthly 8-h max O_3 concentrations in urban and peri-urban sites in the NYC metropolitan area during 2007–2017. The declining trends in peri-urban sites are consistent with national O_3 trends for less urbanized and rural areas [12]. These sites are usually located downwind of urban agglomerations where the highest 8-h max O_3 concentrations were historically recorded. Conversely, an increasing trend of O_3 was observed for the sites located within the urban agglomeration, areas that historically experienced high traffic-related NO_x emissions and low O_3 concentrations. This is also in agreement with increasing trends at urbanized locations across the US [12]. Similar trends were observed across the world with increasing concentrations in urban areas (0.31 ppbv/year) and declining O_3 levels in rural areas (-0.23 ppbv/year) over the past three decades [28,29]. The opposite trends in O_3 concentrations in peri-urban and urban sites can be tentatively explained by declining anthropogenic VOCs and NO_x emissions over the past decades, and the non-linear sensitivity of O_3 formation to VOCs-to- NO_x instantaneous ratio [30]. In urban areas, O_3 levels are conditioned by NO (from vehicular emission) titration in the early morning. Because of the significant declines in NO_x emissions, titration of O_3 by NO was reduced leading to an increase of nighttime carryover O_3 [30]. Ninneman and Jaffe [21] computed that the summertime ozone production efficiency in New York State rural sites increased in response to NO_x reductions in NO_x -limited conditions. The VOCs-to- NO_x ratio between 2008 and 2017 (based on EPA NEI) may have increased from 26.7% to 83.5% depending on VOCs composition that can transition from VOC-limited conditions to NO_x -limited for O_3 formation. Using satellite measurements of HCHO and NO_2 , Jin et al. [15] estimated that transition from VOCs-limited to NO_x -limited conditions occurred within 40–60 km for NYC by 2013–2016, as compared to 80–120 km in the past, accompanied by the reversal of O_3 weekend effect.

The transition from VOCs-limited to NO_x -limited conditions may be better delineated in O_3 weekend effect. The average OWE effect for the urban areas was consistent with that observed in other US urban areas [31]. It has been attributed to the reduction in NO_x emissions from road traffic on weekends, particularly on Sundays, leading to a lower O_3 titration by NO that also appears to be the dominant cause in NYC. VOCs emissions from recreational and residential activities may offset reduced traffic-related VOCs emissions in weekends allowing for longer O_3 accumulation and production [11]. In peri-urban sites, there was no O_3 weekend effect, in agreement with previous studies [30,31]. This was ascribed to the reduced NO titration throughout the week. Analysis of the 2018 summer O_3 exceedances in NYC, accompanied by a series of heatwaves showed that shortly downwind of Manhattan and within the urban corridor, O_3 formation transitioned to NO_x -limited

conditions. Moreover, the combination of NO_x and biogenic VOCs primarily contributed to high O_3 levels [32].

We observed a strong correlation between O_3 levels and the frequency of regional wildfires. Changes in local photochemistry and regional transport may also influence O_3 trends. For the Northeastern US, ambient ozone concentrations were more dependent on ambient temperature (30%) than anthropogenic NO emissions reductions (10%) [33]. For the Northeast, which includes the study area, regional O_3 transport (60%) explained most of the O_3 variability [33]. Transport from wildfires can modify O_3 at receptor sites. It was previously observed that the 8-h max O_3 concentration increased as the fire intensity increased due to the mixing of VOCs-rich wildfire plumes with NO_x [11,18,24]. These conditions may further enhance the NO_x limited conditions in NYC yielding high O_3 concentrations. Moreover, oxygenated VOCs released during wildfires (e.g., methoxy phenols) may react with NO_x to form stable peroxyacetyl nitrates (PANs) that permanently remove NO_x and moderate downwind O_3 levels [24,32]. The transition from El Niño to La Niña conditions over periods of two–three years of El Niño–Southern Oscillation (ENSO) is associated with increased wildfires in the US. This may be due to the accumulation of fresh biomass during the El Niño events including invasive grasses that trigger faster wildfire progression. During La Niña conditions in the following years, increased temperatures, reduced precipitation, and drought create conditions that promote fast-spreading wildfires [34].

5. Conclusions

The analysis showed increasing O_3 concentrations in sites within urban agglomerations while O_3 concentrations peri-urban have been declining. This was tentatively assigned to changes in the photochemical regime from VOC-limited to NO_x -limited conditions. The weekend-weekday O_3 pattern indicated that reduced O_3 titration by NO has been declining increasing the nighttime O_3 carryover and promoting longer O_3 accumulation periods. Moreover, a strong correlation of O_3 levels with regional wildfires was computed. This was attributed to increased VOCs emissions and the formation of PANs in the smoke plume during transport and its mixing with ground-level air that can further augment NO_x -limited conditions. The frequency and magnitude of wildfires in the eastern US were related to the sequence of El-Niño and La Niña events, with more lightning-ignited fires during dry periods. To mitigate increasing O_3 levels in densely populated areas, future emission control strategies should also consider the compounding global and regional effects of climate change.

Author Contributions: Conceptualization, I.G.K.; methodology, S.S. and I.G.K.; data curation, formal analysis, S.S.; writing—original draft preparation, S.S.; writing—review and editing, I.G.K.; supervision, I.G.K. All authors have read and agreed to the published version of the manuscript.

Funding: This research was partially funded by the Dean’s Dissertation Award.

Institutional Review Board Statement: Not applicable.

Informed Consent Statement: Not applicable.

Data Availability Statement: Air pollutant data are available on US Environmental Protection Agency Air Data web page https://aqs.epa.gov/aqsweb/airdata/download_files.html (accessed on 1 October 2020).

Conflicts of Interest: The authors declare no conflict of interest. The funders had no role in the design of the study; in the collection, analyses, or interpretation of data; in the writing of the manuscript, or in the decision to publish the results.

References

1. Vicedo-Cabrera, A.M.; Sera, F.; Liu, C.; Armstrong, B.; Milojevic, A.; Guo, Y.; Tong, S.; Lavigne, E.; Kyselý, J.; Urban, A.; et al. Short term association between ozone and mortality: Global two stage time series study in 406 locations in 20 countries. *BMJ* **2020**, *368*, m108. [[CrossRef](#)]
2. Agathokleous, E.; Feng, Z.; Oksanen, E.; Sicard, P.; Wang, Q.; Saitanis, C.J.; Araminiene, V.; Blande, J.D.; Hayes, F.; Calatayud, V.; et al. Ozone affects plant, insect, and soil microbial communities: A threat to terrestrial ecosystems and biodiversity. *Sci. Adv.* **2020**, *6*, eabc1176. [[CrossRef](#)]
3. Badman, D.; Jaffe, E.R. Blood and air pollution: State of the knowledge and research needs. *Otolaryngol. Head Neck Surg.* **1996**, *114*, 205–208. [[CrossRef](#)]
4. Kim, C.S.; Alexis, N.E.; Rappold, A.G.; Kehrl, H.; Hazucha, M.J.; Lay, J.C.; Schmitt, M.T.; Case, M.; Devlin, R.B.; Peden, D.B.; et al. Lung function and inflammatory responses in healthy young adults exposed to 0.06 ppm ozone for 6.6 hours. *Am. J. Respir. Crit. Care Med.* **2001**, *163*, 1215–1221. [[CrossRef](#)] [[PubMed](#)]
5. Khatri, S.; Holguin, F.C.; Ryan, P.B.; Mannino, D.; Erzurum, S.C.; Teague, W.G. Association of ambient ozone exposure with airway inflammation and allergy in adults with asthma. *Asthma* **2009**, *46*, 777–785. [[CrossRef](#)] [[PubMed](#)]
6. Mortimer, K.; Neugebauer, R.; Lurmann, F.; Alcorn, S.; Balmes, J.; Tager, I. Air pollution and pulmonary function in asthmatic children: Effects of prenatal and lifetime exposures. *Epidemiology* **2008**, *19*, 550–562. [[CrossRef](#)] [[PubMed](#)]
7. Nishimura, K.K.; Galanter, J.M.; Roth, L.A.; Oh, S.S.; Thakur, N.; Nguyen, E.A.; Thyne, S.; Farber, H.J.; Serebrisky, D.; Kumar, R.; et al. Early-life air pollution and asthma risk in minority children. The GALA II and SAGE II studies. *Am. J. Respir. Crit. Care Med.* **2013**, *188*, 309–318. [[CrossRef](#)]
8. Enweasor, C.; Flayer, C.H.; Haczku, A. Ozone-Induced Oxidative Stress, Neutrophilic Airway Inflammation, and Glucocorticoid Resistance in Asthma. *Front. Immunol.* **2021**, *12*, 631092. [[CrossRef](#)]
9. Ierodiakonou, D.; Zanobetti, A.; Coull, B.A.; Melly, S.; Postma, D.S.; Boezen, H.M.; Vonk, J.M.; Williams, P.V.; Shapiro, G.G.; McKone, E.F.; et al. Ambient air pollution, lung function, and airway responsiveness in asthmatic children. *J. Allergy Clin. Immunol.* **2016**, *137*, 390–399. [[CrossRef](#)]
10. Rodopoulou, S.; Samoli, E.; Chalbot, M.G.; Kavouras, I.G. Air pollution and cardiovascular and respiratory emergency visits in Central Arkansas: A time-series analysis. *Sci. Total Environ.* **2015**, *536*, 872–879. [[CrossRef](#)] [[PubMed](#)]
11. Kavouras, I.G.; DuBois, D.W.; Etyemezian, V.; Nikolich, G. Spatiotemporal variability of ground-level ozone and influence of smoke in Treasure Valley, Idaho. *Atmos. Res.* **2013**, *124*, 44–52. [[CrossRef](#)]
12. Simon, H.; Reff, A.; Wells, B.; Xing, J.; Frank, N. Ozone Trends Across the United States over a Period of Decreasing NO_x and VOC Emissions. *Environ. Sci. Technol.* **2015**, *49*, 186–195. [[CrossRef](#)]
13. Strode, S.A.; Ziemke, J.R.; Oman, L.D.; Lamsal, L.N.; Olsen, M.A.; Liu, J. Global changes in the diurnal cycle of surface ozone. *Atmos. Environ.* **2019**, *199*, 323–333. [[CrossRef](#)]
14. Henneman, L.R.F.; Shen, H.; Liu, C.; Hu, Y.; Mulholland, J.A.; Russell, A.G. Ozone in the Eastern United States: Production Efficiency Variability Over Time and Between Sources. In *Air Pollution Modeling and its Application XXVI. ITM 2018. Springer Proceedings in Complexity*; Mensink, C., Gong, W., Hakami, A., Eds.; Springer: Cham, Switzerland, 2020; Chapter 9. [[CrossRef](#)]
15. Jin, X.; Fiore, A.; Boersma, K.F.; De Smedt, I.; Valin, L. Inferring Changes in Summertime Surface Ozone–NO_x–VOC Chemistry over U.S. Urban Areas from Two Decades of Satellite and Ground-Based Observations. *Environ. Sci. Technol.* **2020**, *54*, 6518–6529. [[CrossRef](#)]
16. Wells, B.; Dolwick, P.; Eder, B.; Evangelista, M.; Foley, K.; Mannshardt, E.; Misenis, C.; Weishampel, A. Improved estimation of trends in U.S. ozone concentrations adjusted for interannual variability in meteorological conditions. *Atmos. Environ.* **2021**, *248*, 118234. [[CrossRef](#)] [[PubMed](#)]
17. Ren, J.; Hao, Y.; Simayi, M.; Shi, Y.; Xie, S. Spatiotemporal variation of surface ozone and its causes in Beijing, China since 2014. *Atmos. Environ.* **2021**, *260*, 118556. [[CrossRef](#)]
18. Wilkins, J.L.; de Foy, B.; Thompson, A.M.; Peterson, D.A.; Hyer, E.J.; Graves, C.; Fishman, J.; Morris, G.A. Evaluation of Stratospheric Intrusions and Biomass Burning Plumes on the Vertical Distribution of Tropospheric Ozone Over the Midwestern United States. *J. Geophys. Res.* **2020**, *125*, e2020JD032454. [[CrossRef](#)]
19. Jaffe, D.A.; Wigder, N.; Downey, N.; Pfister, G.; Boynard, A.; Reid, S.B. Impact of Wildfires on Ozone Exceptional Events in the Western, U.S. *Environ. Sci. Technol.* **2013**, *47*, 11065–11072. [[CrossRef](#)]
20. U.S. Census Bureau. American Community Survey 5-Year Estimates Data Profiles. 2019. Available online: <https://data.census.gov/cedsci/table?tid=ACSDP5Y2019.DP05&g=310XX00US35620>. (accessed on 10 December 2021).
21. Ninneman, M.; Jaffe, D. Observed Relationship between Ozone and Temperature for Urban Nonattainment Areas in the United States. *Atmosphere* **2021**, *12*, 1235. [[CrossRef](#)]
22. United States Environmental Protection Agency Air Data. Pre-Generated Data Files. Available online: https://aqsweb.airdata/download_files.html#Daily (accessed on 8 October 2021).
23. National Interagency Fire Center. Statistics. Available online: <https://www.nifc.gov/fire-information/statistics> (accessed on 10 December 2021).
24. Chalbot, M.C.; Kavouras, I.G.; Dubois, D.W. Assessment of the Contribution of Wildfires to Ozone Concentrations in the Central US-Mexico Border Region. *Aerosol Air Qual. Res.* **2013**, *13*, 838–848. [[CrossRef](#)]

25. Sather, M.E.; Cavender, K. Update of Longterm Trends Analysis of Ambient 8-hour Ozone and Precursor Monitoring Data in the South Central U.S.; Encouraging News. *J. Environ. Monit.* **2012**, *14*, 666–676. [[CrossRef](#)] [[PubMed](#)]
26. Shikwambana, L.; Mhangara, P.; Mbatha, N. Trend Analysis and First Time Observations of Sulphur Dioxide and Nitrogen Dioxide in South Africa Using TROPOMI/Sentinel-5 P Data. *Int. J. Appl. Earth Obs. Geoinf.* **2020**, *91*, 102130. [[CrossRef](#)]
27. Opio, R.; Mugume, I.; Nakatumba-Nabende, J. Understanding the Trend of NO₂, SO₂ and CO over East Africa from 2005 to 2020. *Atmosphere* **2021**, *12*, 1283. [[CrossRef](#)]
28. Sicard, P.; Paoletti, E.; Agathokleous, E.; Araminienè, V.; Proietti, C.; Coulibaly, F.; De Marco, A. Ozone weekend effect in cities: Deep insights for urban air pollution control. *Environ. Res.* **2020**, *191*, 110193. [[CrossRef](#)] [[PubMed](#)]
29. Sicard, P. Ground-level ozone over time: An observation-based global overview. *Curr. Opin. Environ. Sci. Health* **2021**, *19*, 100226. [[CrossRef](#)]
30. Yan, Y.; Lin, J.; He, C. Ozone trends over the United States at different times of day. *Atmos. Chem. Phys.* **2018**, *18*, 1185–1202. [[CrossRef](#)]
31. Baidar, S.; Hardesty, R.M.; Kim, S.-W.; Langford, A.O.; Oetjen, H.; Senff, C.J.; Trainer, M.; Volkamer, R. Weakening of the weekend ozone effect over California's South Coast Air Basin. *Geophys. Res. Lett.* **2015**, *42*, 9457–9464. [[CrossRef](#)]
32. Coggon, M.G.; Gkatzelis, G.I.; McDonald, B.C.; Gilman, J.B.; Schwantes, R.H.; Abuhassan, N.; Aikin, K.C.; Arend, M.F.; Berkoff, T.A.; Brown, S.S.; et al. Volatile chemical product emissions enhance ozone and modulate urban chemistry. *Proc. Natl. Acad. Sci. USA* **2021**, *118*, e2026653118. [[CrossRef](#)]
33. Kerr, G.H.; Waugh, D.W.; Sarah, S.A.; Steenrod, S.D.; Oman, L.D.; Strahan, S.E. Disentangling the drivers of the summertime ozone-temperature relationship over the United States. *J. Geophys. Res. Atmos.* **2019**, *124*, 10503–10524. [[CrossRef](#)]
34. Mason, S.A.; Hamlington, P.E.; Hamlington, B.D.; Matt Jolly, W.; Hoffman, C.M. Effects of climate oscillations on wildland fire potential in the continental United States. *Geophys. Res. Lett.* **2017**, *44*, 7002–7010. [[CrossRef](#)]